THREE-DIMENSIONAL MHD MODELS OF WAVES IN ACTIVE REGIONS: APPLICATION TO CORONAL SEISMOLOGY

J. A. McLaughlin and L. Ofman

The Catholic University of America, NASA Goddard Space Flight Center, Code 612.1, Greenbelt MD, 20771, USA
james@lssp-mail.gsfc.nasa.gov

ABSTRACT

We present results from three-dimensional MHD simulations of the behavior of MHD waves in 3D models of coronal active regions and loops. The models of the active regions are constructed by using a dipole magnetic field, and gravitationally stratified coronal density structure. We compare the main features of the model with those seen recently by the SOHO and TRACE satellites and investigate the application of the results to coronal seismology. We discuss the possible application of STEREO data to the improvement of our model.

Key words: Coronal active regions; Coronal loops; MHD; Waves; STEREO.

1. INTRODUCTION

Active regions (ARs) are magnetic structures in the solar corona associated with areas of concentrated magnetic field, increased temperature and density and are dynamic in nature. At this time, the dynamics, heating and stability of ARs are not yet fully understood. The behavior of perturbations and waves in ARs depend upon many factors, such as the magnetic field strength, local topology, temperature and density. Recent observations of wave activity in EUV by the SOHO and TRACE satellites, coupled with measurements of photospheric magnetograms and three-dimensional numerical models have improved our understanding of active regions. The detection of these coronal waves and three-dimensional modeling provides us with a new diagnostic tool for obtaining the parameters of the corona; **coronal seismology**.

In this paper, we focus on the behavior of MHD waves in active regions, for which waves are observed in EUV by TRACE and EIT by SOHO. Despite the complexity of the damped 3D modes observed, theoretical models of the local interaction of waves with coronal structures has been performed (Uchida 1968; 1970; Ofman & Thompson 2002; Terradas & Ofman 2004; Ofman 2005; 2006).

We have performed simulations of three-dimensional MHD wave propagation in models of coronal active regions. Here, we present descriptions of the methodology and techniques that are used in the construction of such simulations. These include:

- The MHD equations solved and the velocity perturbations used to simulate, for example, incoming EIT waves.
- The construction of the active region model using extrapolations of the observed photospheric magnetic field and gravitational stratification of the coronal density structure.
- The inclusion of the density structure of individual, realistic coronal loops using a new technique.

In Section 4, we present the numerical results of a fast magnetoacoustic wave impacting on a 3D dipole with an over-dense loop in the system, and compare it to the original system of Ofman & Thompson (2002).

2. MHD EQUATIONS AND MODEL

We solve the three-dimensional, non-linear, resistive MHD equations, including gravitational effects.

$$\begin{aligned} \frac{\partial \rho}{\partial t} + \nabla \cdot (\rho \mathbf{v}) &= 0 \,, \\ \rho \left[\frac{\partial \mathbf{v}}{\partial t} + (\mathbf{v} \cdot \nabla)\, \mathbf{v} \right] &= -\frac{\beta}{2} \nabla p - \frac{1}{F_r r^2} \\ &+ (\nabla \times \mathbf{B}) \times \mathbf{B} \,, \\ \frac{\partial \mathbf{B}}{\partial t} &= \nabla \times \left(\mathbf{v} \times \mathbf{B} - \frac{1}{S} \nabla^2 \mathbf{B} \right) \,, \end{aligned} \tag{1}$$

where $\mathbf{v}$ is fluid velocity, ρ is density, p is pressure and $\mathbf{B}$ is the magnetic induction (usually called the magnetic field). Furthermore, $F_r = \frac{V_A^2 R_s}{G M_s}$ is the Froude number, G is the gravitational constant, M_s is the solar mass, $\beta = \frac{2 c_s^2}{\gamma V_A^2}$ is the ratio of the thermal to the magnetic pressure, c_s is the sound speed, V_A is the Alfvén speed, and S is the Lundquist number.

Proc. SOHO 17 – 10 Years of SOHO and Beyond, Giardini Naxos, Sicily, Italy
7 – 12 May 2006 (ESA SP-617, July 2006)

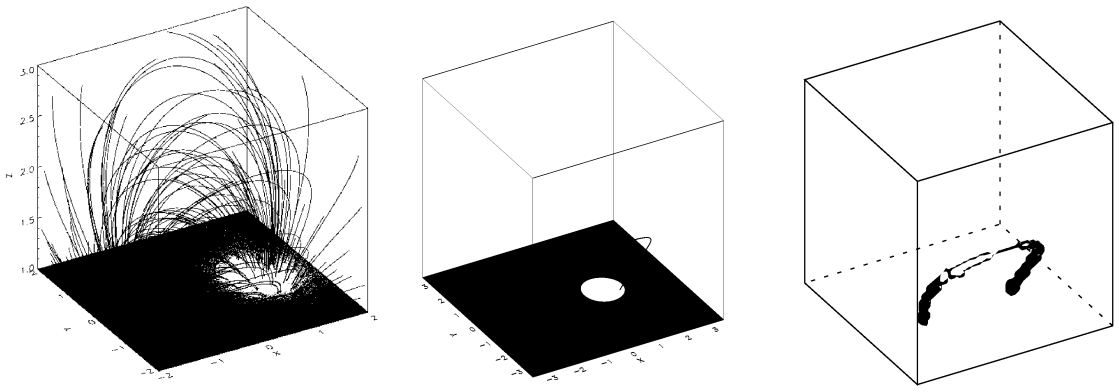

Figure 1. (Left) Our initial 3D magnetic field configuration. (Middle) We select a fieldline from our field extrapolation. (Right) Stratified density is added along the loop length.

At present, we are studying the isothermal case; $\gamma = 1$, $T_0 = 10^6\ K$. The equations are solved with a modified *Lax-Wendroff* scheme with a fourth-order smoothing term. The divergence of the magnetic field is corrected with *Powel's method*. Details of the numerical code can be found in Ofman & Thompson (2002).

2.1. Boundary and Initial Conditions

At the base of the corona, we keep the magnetic field fixed while we use zero-order extrapolation for the velocity and density. We use open boundary conditions for all the variables at the other five planes (i.e. extrapolated variables).

We take an idealized 3D dipole as our initial magnetic field configuration. This can be seen in the left-hand subfigure of Figure 1. We also assume a gravitationally stratified equilibrium density, given by:

$$\rho(x,y,z,0) = \rho_0 \exp H \left[\frac{1}{(10 + z - z_{\min})} - \frac{1}{10} \right] , \quad (2)$$

where H is the normalized scale height.

$$H = \frac{2k_B T}{G M_s m_p} \frac{R_s}{10} . \quad (3)$$

TRACE has provided high-cadence observations of AR distortion due to EIT waves (Wills-Davey & Thompson 1999) and resulting coronal loop oscillations (Aschwanden et al. 1999, Nakariakov et al. 1999, Verwichte et al. 2004). We can recreate these phenomena in our simulations. Below, we model the propagation of a fast magneto-acoustic wave interacting with our simulated AR by sending a velocity pulse in from one of the boundary planes:

$$v_y = A V_A(x,z) \quad \text{for } 0 \le t \le 10\tau_A \quad (4)$$

where A is the initial amplitude of the pulse ($A = 0.25$) and V_A is the local Alfvén speed. We take the magnetic field strength of the dipole to be 85 Gauss, temperature $T = 10^6 K$ and density $10^9 \mathrm{cm}^{-3}$, corresponding to an (isothermal) sound speed of $128.5 \mathrm{kms}^{-1}$. The velocities are normalized by the Alfvén speed $V_{A0} = 3587 \mathrm{kms}^{-1}$ and time is normalized by the Alfvén time $\tau_A = 10\mathrm{s}$. The Lundquist number is set to $S = 10^4$.

3. MASS-BEARING LOOPS

It has been noted that the observed coronal loop oscillations are rapidly damped within a few wave periods. There are several proposed theories to explain this damping, including enhanced viscosity (Nakariakov et al. 1999), wave leakage (Terradas et al. 2005) and resonant absorption (Ruderman & Roberts 2002). By adding more realistic loop structure to our AR loops, we will be able to investigate the relative importance of the above mechanisms.

We see dense loops in the corona (e.g. in observations taken by TRACE) and these structures persist for long periods of time. Hence, the inclusion of over-dense loops is a natural extension to the modeling of active regions. Previous models of coronal loops have used analytical density profiles in the set-up of their systems, e.g. circular and elliptical loops. Here, we choose individual fieldlines and increase the density along them. This will modify the Alfvén speed in that loop. We are also extending this technique to include more complicated loop structures, such as a non-uniform density across the loop. In order to create a steady state, the density in these loops must satisfy the momentum balance equation:

$$\frac{\beta}{2} \nabla p + \frac{\rho}{F_r r^2} - (\nabla \times \mathbf{B}) \times \mathbf{B} = 0 . \quad (5)$$

So we need to create a (self-consistent) density structure to do this. If we do not satisfy equation (5), the material in the loop will drain down due to gravity and pressure imbalance. However, in this paper we impose the over-dense loop as an initial condition in our system and artificially hold it in place. This is analogous to adding

an artificial force to equation (5) and this force can be thought of as a replenishing term or a heating term. This method keeps the loop steady. Holding the loop in place like this is not consistent with satisfying equation (5), but does provide a good first attempt at understanding the difference between the original system (the system studied in Ofman & Thompson 2002) and the addition of over-dense loops to that system. Our technique consists of choosing a 1D fieldline from our potential field extrapolation and then mapping it onto our 3D numerical grid. This can be seen in middle and right-hand panels of Figure 1. In this paper, the model we present consists of a single mass-loaded fieldine, where the fieldine passes through the point $(x, y, z) = (0, -2.5, 2.5)$. Along this fieldline, we have imposed a density enhancement of ten times the background (stratified) density.

4. NUMERICAL RESULTS

The temporal evolution of the velocity components, perturbed magnetic field and perturbed density components at a point located at $(x, y, z) = (0, -2.5, 2.5)$ in the model are shown in Figure 2. The components denoted in blue correspond to the original system of Ofman & Thompson (2002) and the red quantities show the components at the same point in the mass-loaded loop system. Note this point, $(x, y, z) = (0, -2.5, 2.5)$, is a point actually on our over-dense fieldine.

We can see the response of these perturbed components to the propagation of the wave in the system. Note that because we have taken a point along the $x = 0$ plane and that our idealised system is symmetric about this plane, the perturbations in V_x, B_y and B_z is very small.

The maximum height of the V_y component in the original system is 0.0097 and the maximum height in the mass-loaded system is 0.0093 (at the point $0, -2.5, 2.5$). This corresponds to a 4.8% drop in amplitude. Secondly, the second peak in V_y is 0.0064 for the original system compared to 0.0055 in the mass-loaded system (a 13.7% decrease in amplitude). This corresponds to a damping time of $89.1\tau_A$ in the original system and $72.5\tau_A$ in the mass-loaded system.

5. CONCLUSIONS

We have studied the behavior of a fast magnetoacoustic wave propagating towards and inside a simulated active region, constructed from a three-dimensional dipole magnetic configuration. We have presented a comparison between the temporal evolution of the velocity, perturbed magnetic field and perturbed density in a system with a mass-loaded loop and one without.

We find that the temporal evolution of these quantities is similar in both systems. In the mass-loaded loops model, the V_y velocity component is 4.8% less in amplitude than in the original system. Since the density in the mass-loaded system at the point $(x, y, z) = (0, -2.5, 2.5)$ is ten times that of the original system, the Alfvén speed is $\sqrt{10}$ smaller at that point. So a drop in amplitude is not unexpected. Numerical dissipation is also present, but this should be identical in both systems. Despite this, the drop in speed is far less than that which is predicted by idealized single loop studies (e.g. Ofman 2005). This is possibly due to the loop not being fully resolved in the model.

We note that including the over-dense loop has increased the damping rate. This is interesting as it has been noted that observed coronal loop oscillations are rapidly damped within a few wave periods. Thus, there are some interesting features that show potential for this mass-loaded model. Thus, we conclude that it is worthwhile to continue modeling over-dense loops in our model, but that our attempt presented here lacks the sophistication required to fully understand the system, i.e. increasing the density only on the fieldline is insufficent; the internal structure must also be considered. We are currently extending our model to include internal loop structure.

In conclusion, active region wave observations combined with three-dimensional theoretical modeling can be used as a wave diagnostic for coronal parameters. However, all observations are currently confined to line-of-sight imaging. The new STEREO spacecraft will provide stereoscopic information on the solar corona, and the resulting reconstruction will give three-dimensional information on the loop structure. These new observations will allow new comparisons between the data and theory, and will further the development of this diagnostic tool for coronal active region parameters.

ACKNOWLEDGMENTS

The author wishes to thank Jaume Terradas and Barbara Thompson for helpful discussions. This work has been supported by the NASA SR & T grant.

REFERENCES

Aschwanden,M. J., Fletcher,L.,Schrijver,C. J.,Alexander, D. (1999) *ApJ* **520**, 880-

Aschwanden, M. J. De Pontieu, B., Schrijver, C. J., Title, A. (2002) *Sol. Phys* **206**,

Nakariakov, N. M., Ofman, L., DeLuca, E., Roberts, B., Davila, J.M. (1999) *Science* **285**, 862-

Ofman, L., Thompson, B. J. (2002) *APJ* **574**, 440-

Ofman, L. (2005) *Advances in Space Research* **36**, 1572-1578

Ofman, L. (2006) *ApJ* submitted

Ruderman, M. S., Roberts, B. (2002) *ApJ* **577**, 475-

Terradas, J., Ofman, L. (2004) *SOHO 13 Proceedings*, p. 269-472

Terradas, J., Oliver, R., Ballester, J. L. (2005) *ApJ* **618**, L149-

Uchida, Y. (1968) *Sol. Phys* **4**, 30-

Uchida, Y. (1970) *PASJ* **22**, 341-

Verwichte, E., Nakariakov, V. M., Ofman, L. DeLuca, E. E. (2004) *Sol. Phys* **223**, 77-

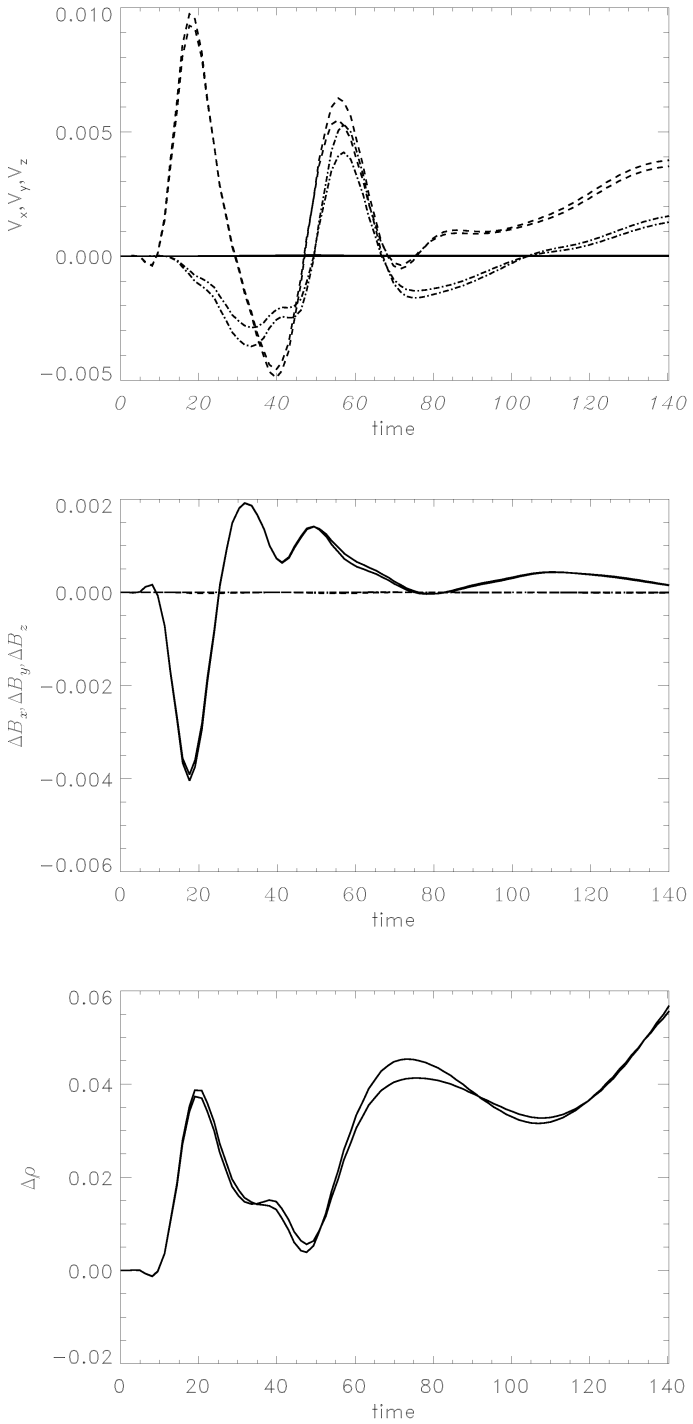

Figure 2. Comparison of the temporal evolution of several quantities between the original system (shown in blue) of Ofman & Thompson (2002) and the simulation with the mass-loaded loop (shown in red), at the point $x = 0.0$, $y = -2.5$, $z = 2.5$. *Upper panel shows the temporal evolution of the velocity components (*V_x*: solid line,* V_y*: dashed line,* V_z*: dash-dotted line), middle panel shows the perturbed magnetic field components (*ΔB_x*: solid line,* ΔB_y*: dashed line,* ΔB_z*: dash-dotted line) and the lower panel shows the perturbed density.*